J Electroceram (2006) 17:235–240
DOI 10.1007/s10832-006-9766-7

Diluted magnetic semiconductor properties of $Zn_{1-x}Co_x$ O: 1 at% Al thin films prepared by pulsed DC magnetron sputtering

Young-Sung Kim · Yoon-Duk Ko · Weon-Pil Tai

Received: 28 June 2005 / Revised: 18 April 2006 / Accepted: 12 July 2006

Abstract Zn_{1-x} Co_xO: 1 at% Al($x = 0 - 0.3$) films were grown on corning 7059 glass by asymmetrical bipolar pulsed dc magnetron sputtering. The c-axis orientation along the (002) plane was enhanced with increasing Co concentration. The ZnCoO thin films are grown to the fibrous grains of tight dome shape. The transmittance spectra showed that sp-d exchange interactions and typical d-d transitions become activated with increasing Co concentration. The electrical resistivity of ZnCoO films increased ranging from $\sim 10^{-3}$ to $\sim 10^{-2}$ Ω·cm with increasing Co concentration, especially it increased greatly at 30 at% Co. X-ray photoelectron spectroscopy and alternating gradient magnetometer analyses indicated that no Co metal cluster in the ZnCoO films is formed and room temperature ferromagnetism is exhibited. These electrical and magnetic properties of ZnCoO films suggest a potential application of dilute magnetic semiconductor devices.

Keywords ZnCoO thin films · Pulsed DC magnetron sputtering · Ferromagnetism · DMS

1 Introduction

Recently, there has been a great deal of interest in the area of spintronics because of developments in the physics of spin-dependent phenomena and their potential technological applications. Diluted magnetic semiconductors (DMS) are therefore extensively studied as potential spintronics materials and expected to play an important role in magnetic, magneto-optical and magneto-electrical fields.

Many researchers tried spin injection into non-magnetic semiconductors due to the potential to create new classes of spintronics devices. Though Ohno et al., succeeded in synthesizing Mn-doped III–V based ferromagnetic semiconductors such as InMnAs and GaMnAs[1, 2], the highest Curie temperature (T_C) of these materials was limited to only 110 K which is far from practical device applications. For practical applications, room temperature ferromagnetic DMS are required and ZnO has recently been employed as host materials for realizing wide-band gap DMS. ZnO-based heterostructures have been investigated for their applications to optoelectronic devices because of its high optical transparency in the visible range and good electrical conductivity achievable by appropriate impurity doping. Dietl et al., theoretically proposed that Mn-doped ZnO could achieve high T_C well above room temperature [3]. In addition, Sato et al., theoretically suggested that the ferromagnetic state in Mn, Fe, Co and Ni doped ZnO-DMS can be stabilized [4, 5]. Ueda et al., experimentally reported the ferromagnetic behaviors with a Curie temperature higher than room temperature for the Co-doped ZnO films [6]. Recently, Yang et al., succeeded in obtaining room temperature ferromagnetism of which Curie temperature is higher than 350 K by RF sputtering [7] and it could provide the practical applications of room temperature DMS devices.

Several techniques such as sputtering [8], PLD (pulsed laser deposition) [9], MBE, and sol-gel [10] method have been employed for preparing transition metal-doped ZnO films. However, bipolar pulsed DC magnetron sputtering process has been seldom tried for the preparation of ZnO based DMS materials.

Y.-S. Kim (✉) · Y.-D. Ko
Advanced Material Process of Information Technology,
Sungkyunkwan University, Suwon 440-746, Korea
e-mail: youngsk@skku.edu

W.-P. Tai
Fine Chemical Industry Support Center, Ulsan Industry,
Promotion Techno Park, Ulsan 683-804, Korea

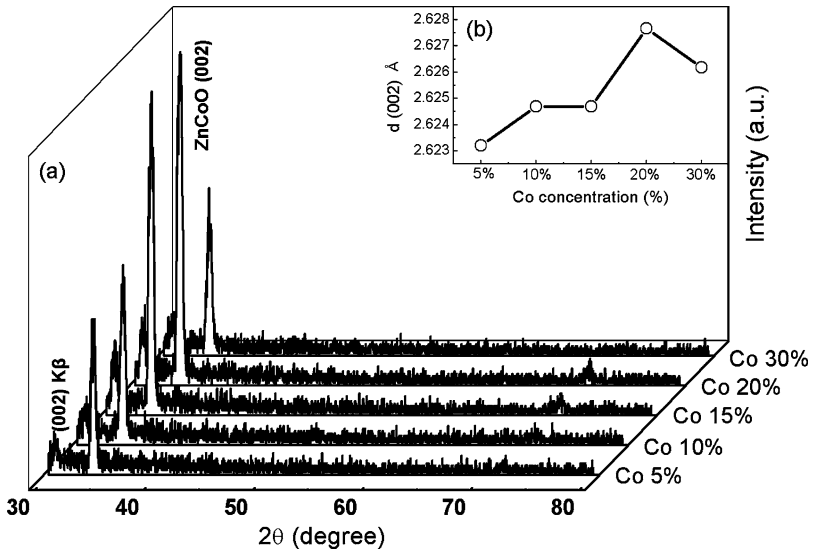

Fig. 1 XRD patterns (a) and d-spacings (b) of ZnCoO thin films with Co concentration

In this study, we have prepared Co-doped ZnO thin films with different Co concentration on glass by bipolar pulsed DC magnetron sputtering method and investigated the magnetic and electrical properties of the films.

2 Experiment

$Zn_{1-x}Co_xO$: 1 at% Al ($x = 0 - 0.30$) films were grown on corning 7059 glass by asymmetrical bipolar pulsed DC magnetron sputtering. The sputtering target was fabricated by sintering 99.0 at% ZnO, 1.0 at% Al and x% CoO ($x = 0 - 0.30$). Al was added to the targets at 1 at% as a stabilizer to control electron concentration in the ZnO thin films [11]. Because the pure ZnCoO films show very unstable the electrical properties for specific resistance, which are above three orders of magnitude higher and it also is very difficult to control them in our advanced experiments. The sputtering chamber was pumped down to 5×10^{-6} Torr by turbo molecular pump and Ar gas was only used as a sputtering gas. The target was pre-sputtered by Ar plasma for 5 min to clean the target. The thickness of the films was deposited in the range of 250–300 nm on the base of the deposition rate which is obtained from SEM cross section.

The crystallographic structure of ZnCoO thin films was investigated by the HRXRD (high resolution x-ray diffraction, Bruker AXS, D8 Discover). The surface morphology and thickness of films were observed by ESEM (environmental scanning electron microscope, Philips, XL30 ESEM-FEG). The resistivity, carrier concentration and Hall mobility of the films were investigated by van der Pauw method through Hall measurement (Hall effect measurement system, ECOPIA, HMS-3000). The optical transmittance of ZnCoO thin films were measured by UV-vis. spectrometer (Spectro Photometa U3000, Hitachi) and optical band gap was calculated. The magnetic properties were examined using an alternating gradient magnetometer (AGM, Princeton Measurements, 2900–02) system at room temperature.

3 Results and discussion

Because (002) plane in hexagonal wurtzite ZnO has the lowest surface energy due to the high atomic packing factor, ZnO thin films are c-axis oriented [12, 13]. In this work, *c*-axis oriented ZnCoO thin films are deposited with Co concentration and the appropriate temperature and pulse frequency conditions are determined by pre-experiments [11].

The crystal orientation and crystallinity of the ZnCoO films with different Co concentration were determined by HRXRD. Figure 1 shows the HRXRD patterns and d-spacings for the (002) plane in the ZnCoO films. The *c*-axis oriented ZnCoO films were grown well for all the Co concentration and any secondary peaks did not appear. The XRD patterns also indicate that the Co doping does not change the wurtzite structure of ZnO for doping concentrations below 30 at%. The peak intensity of the (002) plane increases with increasing Co concentration in the range of 5–20 at%, but it decreases at the Co concentration of 30 at%. When 20 at% Co was doped with ZnCoO thin films, the peak intensity of the (002) plane had the highest value. It indicates that a highly *c*-axis preferred films were grown at the concentration of 20 at% Co. The d-spacing value of (002) plane in the ZnCoO films increases with increasing Co concentration in the range of 5–20 at%, as shown in Fig. 1(b). The increased d value with increasing Co concentration is due to the Vegard law. In our study, however, the d value slightly decreases at 30 at% Co. It is concluded that the solubility of Co exceeds a thermal equilibrium limit above 30 at% Co and the crystallinity of ZnCoO thin films is decreased.

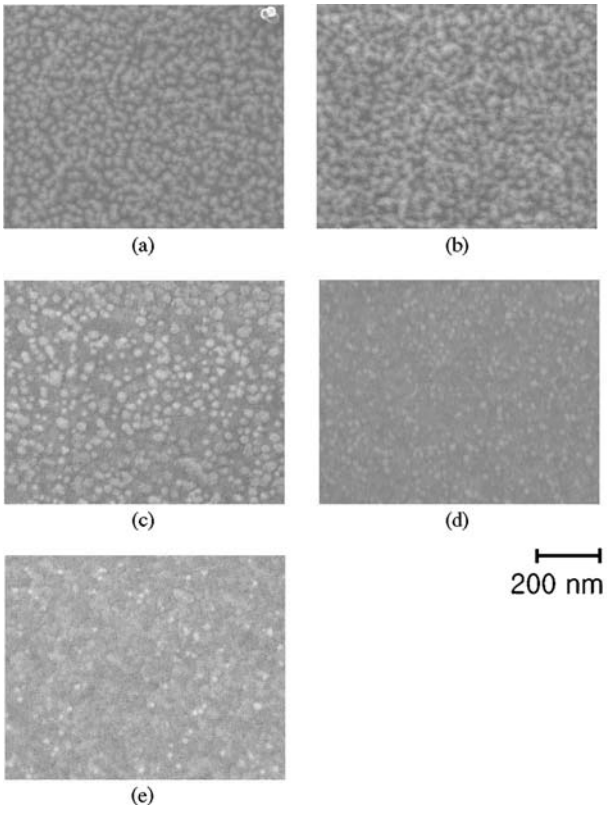

Fig. 2 SEM micrographs of ZnCoO thin films with Co concentration: (a) 5 at%, (b) 10 at%, (c) 15 at% (d) 20 at% and (e) 30 at%

Figure 2 shows the surface morphologies of ZnCoO films as a function of Co concentration. All the films have tightly packed grains and relatively smooth surface and the grains are grown in the form of nano size structure. The morphologies of the films are in agreement with the trend given by Thornton's structure zone model. In the structure zone model, the surface structure was classed in terms of four zones as function of T/Tm and argon pressure, where both T and Tm are substrate temperature and coating material melting point, respectively. In our study, the morphologies of ZnCoO thin films have tightly packed fibrous grains and relatively smooth domed surface is observed at T/Tm = 0.34 and Ar pressure = 5 mTorr [14].

Figure 3 shows the chemical bonding states of Co in the ZnCoO thin films with Co concentration. The charge shifted spectra was corrected from the adventitious C_{1s} photoelectron signal at 284.5 eV [15]. In our study, the energy difference between $Co_{2p1/2}$ and $Co_{2p3/2}$ is 15.5 eV. If Co exists as a metal cluster in the ZnCoO thin films, the energy difference should be 15.05 eV. On the contrary, these differences should be 15.5 eV when Co is bonding with oxygen [16]. As a result, the formation of Co cluster in the films can be ruled out and Co^{2+} ions possibly occupy the Zn site without changing the wurzite structure.

Figure 4 shows the optical transmittance spectra of ZnCoO thin films with different Co concentration in the wavelength from 200 to 800 nm. The optical transmittance of the films in the visible range is relatively high, and sharp ultraviolet absorption edge at the wavelength of about 368 nm is formed. The transparency of films faded away and the green color overwhelmed with increasing Co concentration [6]. The color of thin films is getting dark due to typical d-d transitions of Co ions. The absorption bands appeared at approximately 568, 615 and 660 nm (2.18, 2.00 and 1.88 eV) are attributed to d-d transitions of high spin states of Co^{2+}ions [17]. The absorption band is determined by the spectroscopy properties of Co^{2+} ions. The Co^{2+} ions in the

Fig. 3 XPS spectra of Co $2p_{1/2}$ and $2p_{3/2}$ peaks for ZnCoO thin films with Co concentration: (a) 5 at%, (b) 10 at%, (c) 15 at% (d) 20 at% and (e) 30 at%

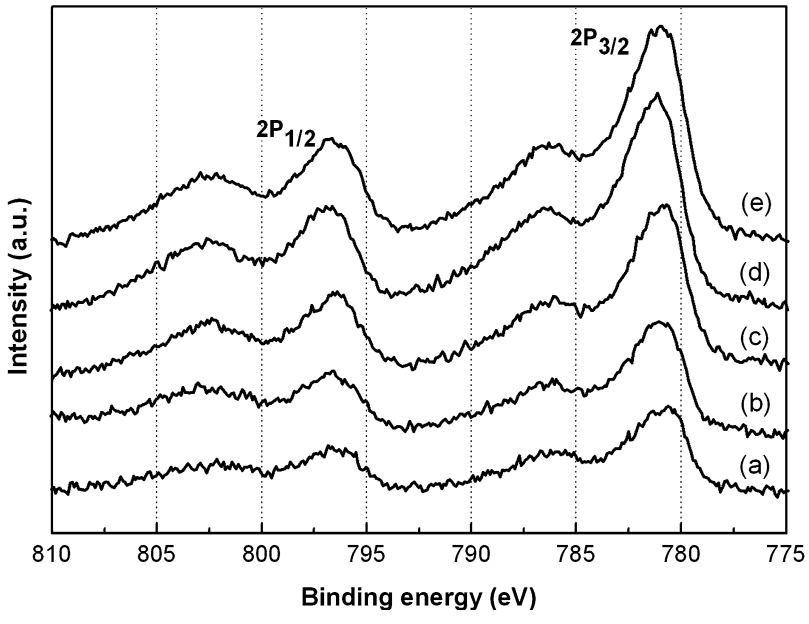

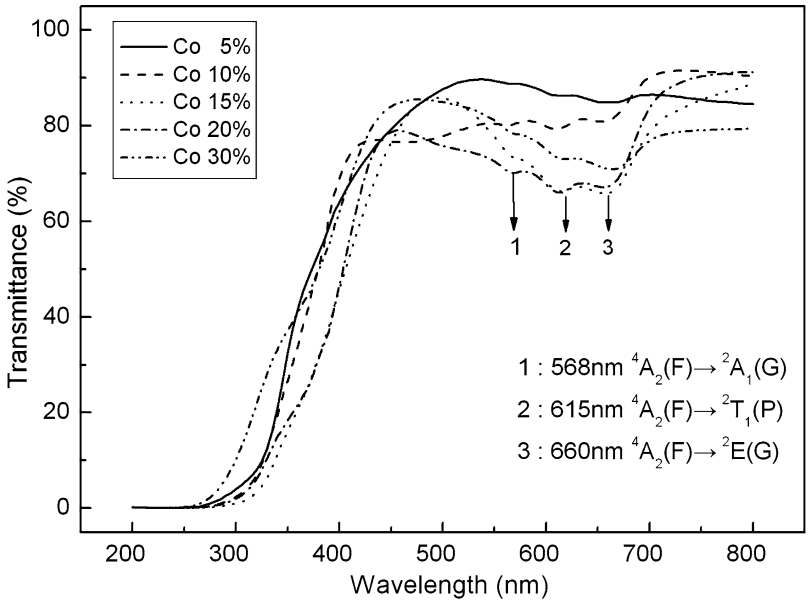

Fig. 4 Optical transmittance spectra of ZnCoO thin films with Co concentration

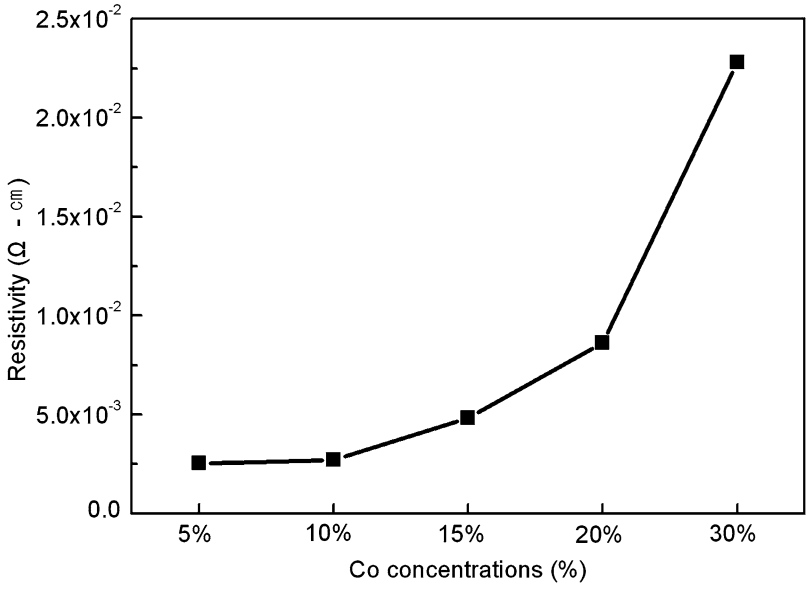

Fig. 5 Resistivity of ZnCoO thin films with Co concentration

ZnCoO thin films have the localized orbit which is singular rotational non-symmetrical state originated from metallic 4f orbit by forming ZnCoO complex compound. The absorption band is ascribed to d-d transition of high spin state of Co^{2+}, which is the electron transition from the localized orbit that has singular rotational non-symmetrical state to the localized orbit which has double symmetrical and non-symmetrical state originated from metallic 2g orbit appeared at 660 nm. This absorption band is inscribed as $^4A_2(F) \rightarrow {}^2E(G)$ by Mulliken spectroscopy sign. The absorption band at 615 nm appeared due to electron transition ($^4A_2(F) \rightarrow {}^2T_1(P)$) from the same initial state to the localized orbit which has triple rotational symmetrical state originated from metallic 2p orbit. The absorption band at 568 nm occurred due to electron transition from the same initial state to the localized orbit which has singular rotational symmetrical state and originated from metallic 2g orbit ($^4A_2(F) \rightarrow {}^2A_1(G)$). Thus, ZnCoO thin films have clear green color because of absorption bands originated from electron transition. The absorption intensity in the films with uniformly controlled thickness enhanced with increasing Co concentration, but it is rather weaken at 30 at% Co. This weakening of absorption band is assigned as the decrease of the solubility at 30 at% Co.

The electrical resistivity of ZnCoO thin films prepared at different Co concentration is shown in Fig. 5. The resistivity of ZnCoO thin films is in the range of 10^{-2}–10^{-3} and it increases gradually with increasing Co concentration

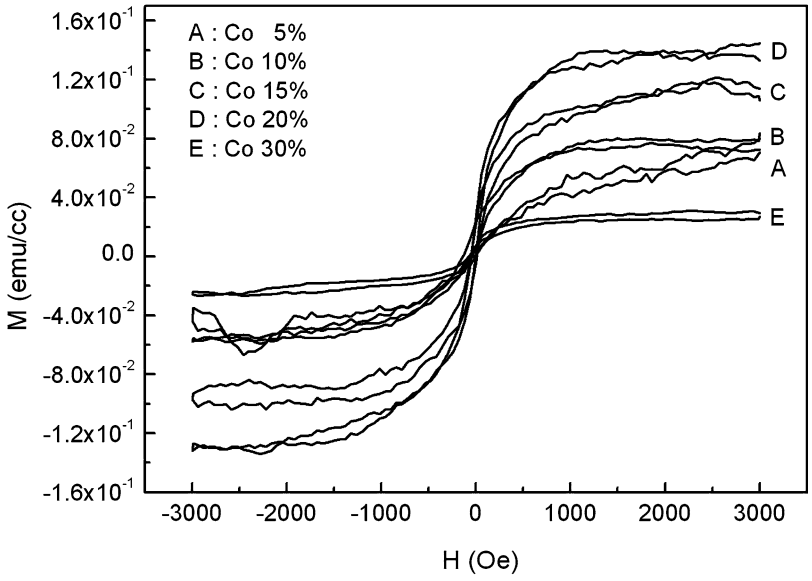

Fig. 6 Magnetization (M) versus magnetic field (H) curves of ZnCoO films measured by AGM system at room temperature

from 5 at% to 30 at%. It was reported that the doping of Al as a stabilizer to control electron concentration in the ZnO thin films enhances the electrical properties because of increased carrier concentration [6]. The decrease of oxygen vacancies and Zn interstitials reduces the carrier concentration because Co^{2+}(0.058 nm) ions systematically substitutes Zn^{2+}(0.06 nm) ions and leading to an increased resistivity of the films. Especially, the resistivity steeply increases at the 30 at% Co due to the decline of crystallinity.

The magnetic properties in the ZnCoO thin films were investigated by AGM at room temperature, as shown in Fig. 6. A well-defined hysteresis loop in the M-H curve indicates the presence of ferromagnetic behaviors at room temperature.

It can be three possible explanation for the origin of ferromagnetism in the ZnCoO thin films. The first possibility is the Co metal cluster [18]. Because Co is ferromagnetic material, it could provide the source of ferromagnetism if it exist in the form of nano-sized cluster. However, the XRD patterns and XPS results apparently indicated that no Co metal cluster exists in our sample. Another possibility is the formation of secondary phases such as CoO because CoO is well-known antiferromagnetic material which has little positive susceptibility. However, this possibility is also excluded because there are no secondary phases in XRD patterns [6]. The carrier-induced ferromagnetism that appeared in II–VI and III–V semiconductors can be a major reason for room temperature ferromagnetism [19, 20]. In this study, ZnCoO thin films have near room temperature ferromagnetism because Co^{2+} ions systematically substitute Zn^{2+} ions. Moreover, the saturation magnetization decreases at 30 at% Co because Co^{2+} ions doped more than thermal equilibrium limit in the films, which correspond with the electrical and optical properties. However, we need to perform further analytical experiments to clarifying the origin of ferromagnetism and electrical properties.

4 Conclusions

ZnCoO thin films were prepared on the glass substrate by a pulsed DC magnetron sputtering. ZnCoO thin films were highly oriented along *c*-axis up to 20 at% Co, but *c*-axis orientation is worsen at 30 at% Co because of thermal equilibrium limit in ZnO thin films. The transmittance spectra showed typical d-d transition between Co^{2+} ions and sp-d exchange interaction in the films. The resistivity of ZnCoO thin films increases with increasing Co concentration due to the decrease of carrier concentration. The room temperature ferromagnetism was enhanced with increasing Co concentration in the range of 5–20 at% Co. However, the saturation magnetization remarkably decreased at the 30 at% Co because the crytallinity of thin films get worsen due to solubility limit in ZnCoO thin films. The ZnCoO thin films with 5–20 at% Co have low resistivity of 10^{-2}–10^{-3} and room temperature ferromagnetism, leading to magnetic semiconductor.

Acknowledgements This work was supported by the Ministry of Commerce, Industry and Energy (MOCIE) through Advanced Material Process of Information Technology (AMPIT) (R12-2002-057-01001-0) and Regional Technological Innovation Program at Sungkyunkwan University (RTI04-03-04).

References

1. H. Ohno, H. Manakata, T. Penney, S. von Molnar, and L.L. Chan, *Phys. Rev. Lett.*, **68**, 2644 (1992).

2. H. Ohno, *Science*, **281**, 951 (1998).
3. T. Dietl, H. Ohno, F. Matsukura, J. Cibert, and D. Ferrand, *Science*, **287**, 1019 (2000).
4. K. Sato and H. Katayama-Yoshida, *Jpn. J. Appl. Phys. Exp. Lett.*, **39**, L555 (2000).
5. K. Sato, H. Katayama-Yoshida, *Physica*, **B308–310**, 904 (2001).
6. K. Ueda, H. Tabata, and T. Kawai, *Appl. Phys. Lett.*, **79**, 988 (2001).
7. S.G. Yang, A.B. Pakhomov, S.T. Hung, and C.Y. Wong, *IEEE Trans. Magn.*, **38**, 2877 (2002).
8. H.J. Kim, I.C. Song, J.H. Sim, H. Kim, D. Kim, Y.E. Ihm, and W.K. Choo, *Phys. Stat. Sol.*, **241**, 1553 (2004).
9. N. Jedrecy, H.J. von Bardeleben, Y. Zheng, and J.-L. Cantin, *Phys. Rev.*, **B69**(041308), 1 (2004).
10. N. Viart, M. Richard-Plouet, D. Muller, and G. Pourroy, *Thin Solid Films*, **437**, 1 (2003).
11. H. Ko, W.P. Tai, K.C. Kim, S.H. Kim, S.J. Suh, and Y.S. Kim, *J. Cryst. Growth*, **277**, 352 (2005).
12. S.H. Jeong and J.H. Boo, *Thin Solid Films*, **447–48**, 105 (2004).
13. J.M. Ting, B.S. Tsai, *Mater. Chem. Phys.*, **72**, 273 (2001).
14. D. Song, A.G. Aberle, and J. Xia, *Appl. Surf. Sci.*, **195**, 291 (2002).
15. J.F. Moulder, et al., *Handbook of X-ray Photoelectron Spectroscopy* (Physical Electronics, Inc., 1992).
16. C.D. Wagner, W.M. Riggs, L.E. Davis, and J.F. Moulder, in *Handbook of X-ray photoelectron Spectroscopy*, edited by G.E. Mulenberg (Perkin-Elmer Co., 1979), p. 78.
17. Z. Jin, M. Murakami, T. Fukumura, Y. Matsumoto, A. Ohtomo, M. Kawasaki, and H. Koinuma, *J. Cryst. Growth*, **214–215**, 55 (2000).
18. J.H. Park, M.G. Kim, H.M. Jang, S. Ryu, and Young M. Kim, *Appl. Phys. Lett.*, **84**, 1338 (2004).
19. H. Munekata, T. Abe, S. Koshihara, A. Oiwa, M. Hirasawa, S. Katsumoto, Y. Iye, C. Urano, and H. Takagi, *J. Appl. Phys.*, **81**, 4862 (1997).
20. S. Koshihara, A. Oiwa, M. Hirasawa, S. Katsumoto, Y. Iye, C. Urano, H. Takgi, and H. Munekata, *Phys. Rev. Lett.*, **78**, 4617 (1997).